Proceedings of the ASME 2010 International Design Engineering Technical Conferences & Computers and Information in Engineering Conference
IDETC/CIE 2010
August 15-18, 2010, Montreal, Quebec, Canada

DETC2010/AVTT-28198

OPTIMAL PLUG-IN HYBRID VEHICLE DESIGN AND ALLOCATION FOR MINIMUM LIFE CYCLE COST, PETROLEUM CONSUMPTION AND GREENHOUSE GAS EMISSIONS

Ching-Shin Norman Shiau
Research Assistant
Mechanical Engineering

Scott B. Peterson
Research Assistant
Engineering and Public Policy

Jeremy J. Michalek*
Associate Professor
Mechanical Engineering
Engineering and Public Policy

Carnegie Mellon University
Pittsburgh, Pennsylvania 15213
* Corresponding Author Email: jmichalek@cmu.edu

ABSTRACT

Plug-in hybrid electric vehicle (PHEV) technology has the potential to help address economic, environmental, and national security concerns in the United States by reducing operating cost, greenhouse gas (GHG) emissions and petroleum consumption from the transportation sector. However, the net effects of PHEVs depend critically on vehicle design, battery technology, and charging frequency. To examine these implications, we develop an integrated optimization model utilizing vehicle physics simulation, battery degradation data, and U.S. driving data to determine optimal vehicle design and allocation of vehicles to drivers for minimum life cycle cost, GHG emissions, and petroleum consumption. We find that, while PHEVs with large battery capacity minimize petroleum consumption, a mix of PHEVs sized for 25-40 miles of electric travel produces the greatest reduction in lifecycle GHG emissions. At today's average US energy prices, battery pack cost must fall below $460/kWh (below $300/kWh for a 10% discount rate) for PHEVs to be cost competitive with ordinary hybrid electric vehicles (HEVs). Carbon allowance prices have marginal impact on optimal design or allocation of PHEVs even at $100/tonne. We find that the maximum battery swing should be utilized to achieve minimum life cycle cost, GHGs, and petroleum consumption. Increased swing enables greater all-electric range (AER) to be achieved with smaller battery packs, improving cost competitiveness of PHEVs. Hence, existing policies that subsidize battery cost for PHEVs would likely be better tied to AER, rather than total battery capacity.

1. INTRODUCTION

Plug-in hybrid electric vehicle (PHEV) technology has been considered a potentially promising near-term route to addressing global warming and U.S. dependency on foreign oil in the transportation sector as the cost and weight of batteries are reduced [1]. PHEVs use large battery packs to store energy from the electricity grid and propel the vehicle partly on electricity instead of gasoline. Under the average mix of electricity sources in the United States, vehicles can be driven with lower operation cost and fewer greenhouse gas (GHG) emissions per mile when powered by electricity rather than by gasoline [2]. PHEVs have the potential to displace a large portion of the gasoline consumed by the transportation sector with electricity, since approximately 60% of U.S. passenger vehicles travel less than 30 miles per day [3]. Several automobile manufacturers have announced plans to produce PHEVs commercially in the future, including General Motors' Chevrolet Volt, which will carry enough battery modules to store 40 miles worth of electricity [4] and Toyota's plug-in version of the Prius, which will carry enough batteries for approximately 13 miles of electric travel [5].

The structure of a PHEV is similar to that of an ordinary hybrid electrical vehicle (HEV), except the PHEV carries a larger battery pack and offers plug-charging capability [6]. PHEVs store energy from the electricity grid to partially offset gasoline use for propulsion. The hybrid drivetrain has several advantages in terms of improving vehicle efficiency. First, the additional electric motor enables the engine to operate at its most efficient load more of the time, utilizing the batteries to smooth out spikes in power demand. Second, having an additional source of power in the form of an electric motor enables designers to select smaller engine designs with higher fuel efficiency and lower torque capabilities. Third, HEV and PHEV powertrains enable energy that is otherwise lost in braking to be captured to charge the battery and enable the engine to be shut off rather than idling when the vehicle is at rest.

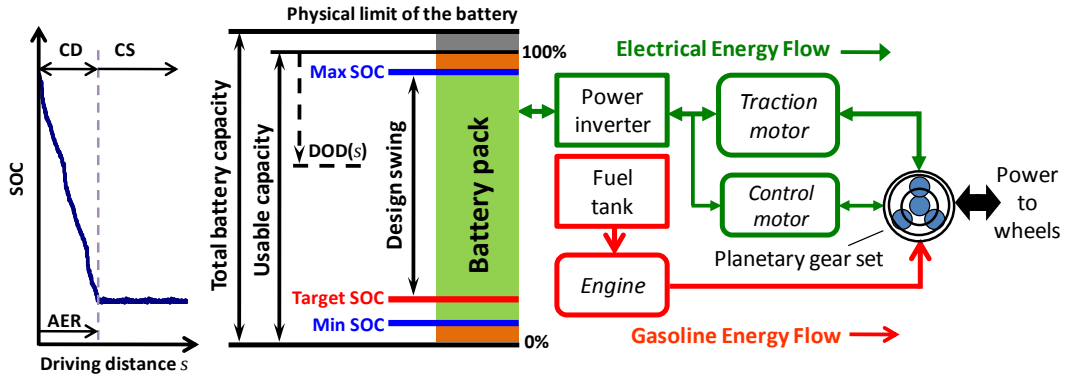

Figure 1. Energy flow in a PHEV with a split powertrain system

We focus on the split configuration in our PHEV study because of its flexibility to perform similarly to a parallel or series drivetrain. The block diagrams in Figure 1 show the structure of the powertrain system in a split PHEV and its energy flow during operation. The system has two energy storage devices – a fuel tank for gasoline and a battery pack for electricity – and three power generation devices – an internal combustion engine, a traction motor and a control motor. The traction motor has higher power output than the control motor and delivers major electrical energy to propel the vehicle. The smaller control motor assists the engine to operate near its optimal efficiency range and balances torque and speed requirements. The power from the engine and motors is coupled by a planetary gear set and then delivered to the wheels. There are two different energy flow paths: electricity energy flow and gasoline energy flow. All electricity flow is bidirectional because the two motors can function as generators.

Our design study focuses on PHEVs with an all-electric control strategy[1], which disables engine operation in charge-depleting mode (CD mode) and draws propulsion energy entirely from the battery until it reaches a target state of charge (SOC), as shown in Figure 1. The distance that a PHEV can travel on electricity alone with a fully charged battery is called its all-electric range (AER).[2] Once the driving distance reaches the AER and the battery is depleted to the target SOC, the PHEV switches to operate in charge-sustaining mode (CS mode), and the gasoline engine provides energy to propel the vehicle and maintain battery charge near the target SOC. In CS mode, the PHEV operates similar to an ordinary HEV.

The battery diagram in Figure 1 presents several definitions relevant to battery capacity. Total battery capacity is determined by the physical charge limits of the battery. Since manufacturing variability implies that every battery cell has a different physical charge limit, battery manufacturers often define 100% SOC at a more controllable level under the upper limit. The capacity window between 0% and 100% defines the usable capacity of the battery. Maximum, target, and minimum SOC are further determined by hybrid vehicle designers based on their design application. We define the capacity window between maximum and target SOC as design swing, and the ratio of discharged capacity to the usable capacity as depth of discharge (DOD), where DOD is a function of driving distance *s*. We further define state of energy (SOE) as the percent of energy remaining in the battery: SOE = energy remaining / energy capacity. If the battery voltage is constant with SOC, then SOC and SOE are equivalent; however, we use SOE in our model to account for voltage variation and focus on the quantity of interest.

Generally, increased AER will result in a larger portion of travel propelled by electrical energy instead of gasoline; however, the distance the vehicle is driven between charges plays an important role in determining the PHEV's advantage: Vehicles that are charged frequently can drive most of their miles on electric power, even with a relatively small battery pack, while vehicles that are charged infrequently require larger battery packs to cover longer distances with electric power [8].

Battery degradation and replacement also affect PHEV implications. Modern batteries have limited life, and frequent cycling leads to accelerated degradation, including reduction in battery capacity and increase in internal resistance caused by the growth of a solid-electrolyte interphase (SEI) layer and a solid film layer on the electrode during battery storage and cycling [9]. A commonly used model of battery degradation views degradation as an increasing function of DOD [10-13], implying that designers should avoid cycling batteries to a deep DOD. However, Peterson et al. [14] used realistic driving cycles to demonstrate that current $LiFePO_4$ battery degrades as a function of energy processed, irrespective of DOD, which has implications for PHEV design.[3] Here we use the Peterson model as a base case and examine DOD-based degradation in a sensitivity analysis.

[1] A blended-strategy PHEV uses a mix of the electric motor and gasoline engine to power the vehicle in CD-mode, while an all-electric PHEV uses only electricity. We confine our scope to all-electric strategy for simplicity, since blended-strategy operation characteristics are sensitive to control parameters.

[2] AER is defined as energy-equivalent electric propulsion distance for blended-mode PHEVs, but we consider only all-electric PHEVs here [7].

[3] This pattern was also observed experimentally by [15].

2. MODEL

We pose a benevolent dictator optimization model to determine optimal vehicle type, design, and allocation for achieving social objectives of minimum equivalent daily cost, life cycle GHG emissions, and petroleum consumption from personal transportation.[4] Figure 2 shows an overview of the modeling framework. For the single vehicle case, the objective function can be expressed as the integral of the corresponding quantity per day at each driving distance $f_O(\mathbf{x},s)$ times the probability distribution of daily driving distances $f_S(s)$ in the population of drivers:

$$\begin{aligned} &\underset{\mathbf{x}}{\text{minimize}} \int_0^\infty f_O(\mathbf{x},s)\, f_S(s)\, ds \\ &\text{subject to } \mathbf{g}(\mathbf{x}) \le \mathbf{0};\ \mathbf{h}(\mathbf{x}) = \mathbf{0} \end{aligned} \tag{1}$$

where $\mathbf{x}$ is a vector of design variables that define the vehicle, s is the distance the vehicle is driven between charges, $f_O(\mathbf{x},s)$ is the value of the objective (equivalent cost, petroleum consumption, or GHG emissions) per day for vehicle design $\mathbf{x}$ when driven s miles per day, $f_S(s)$ is the probability density function for the distance driven per day, $\mathbf{g}(\mathbf{x})$ is a vector of inequality constraints and $\mathbf{h}(\mathbf{x})$ is a vector of equality constraints ensuring a feasible vehicle design.

To extend this model to the case where different drivers are assigned different vehicles based on the distance driven per day, we incorporate a variable s_i that defines the cutoff point such that drivers who travel less than s_i per day are assigned the vehicle defined by $\mathbf{x}_i$ and drivers who travel more than s_i per day are assigned the vehicle defined by $\mathbf{x}_{i+1}$. Extending this idea to multiple segments, the formulation for design and ordered allocation is given by

$$\begin{aligned} &\underset{\mathbf{x}_i, s_i \forall i \in \{1,\ldots,n\}}{\text{minimize}} \sum_{i=1}^{n} \left(\int_{s_{i-1}}^{s_i} f_O(\mathbf{x}_i,s)\, f_S(s)\, ds \right) \\ &\text{subject to } \mathbf{g}(\mathbf{x}_i) \le \mathbf{0};\ \mathbf{h}(\mathbf{x}_i) = \mathbf{0};\ \forall i \in \{1,\ldots,n\} \\ &\qquad s_i \ge s_{i-1};\ \forall i \in \{1,\ldots,n\} \\ &\text{where } s_0 = 0;\ s_n = \infty \end{aligned} \tag{2}$$

In the following subsections, we first instantiate this formulation with specific models for the objective and constraint functions by specifying the distribution of distance driven per day, vehicle performance models, and the objective and constraint formulations.

2.1 Distribution of Vehicle Miles Travelled per Day

We use data from the 2009 National Household Transportation Survey (NHTS) [16] to estimate the distribution of distance driven per day over the population of drivers. The survey collected data by interviewing 136,410 households across the U.S. on the mode of transportation, duration, distance and purpose of the trips taken on the survey day. We fit the weighted driving data using the exponential distribution.[5] The distribution below represents the probability density function for vehicle miles traveled by drivers on the day surveyed:

$$f_S(s) = \lambda e^{-\lambda s};\ s \ge 0 \tag{3}$$

The coefficient λ at maximum likelihood fit is 0.0296. Figure 3 shows the exponential distribution and the histogram of the surveyed daily vehicle driving miles.[6]

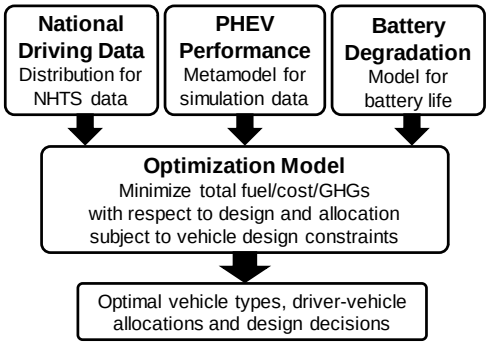

Figure 2. Framework of optimal PHEV design and allocation

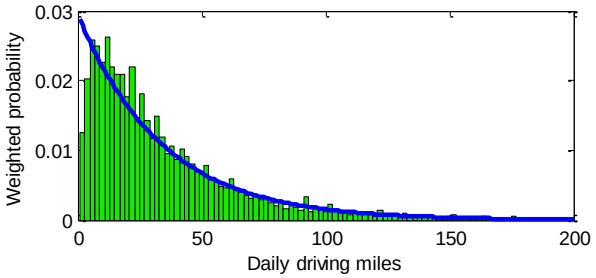

Figure 3. Probability density function for vehicle miles traveled per day

2.2 Vehicle Performance Models

We carry out vehicle performance simulations using the Powertrain System Analysis Toolkit (PSAT) vehicle physical simulator developed by Argonne National Laboratory [17]. PSAT is a Matlab/Simulink forward-looking simulation package that predicts vehicle performance characteristics at both the system level (e.g. fuel consumption) and the component level (e.g. engine torque and speed at each time step) over a given driving cycle using a combination of first principles and empirical component data. In our study, the body, powertrain and vehicle parameters for all PHEV and HEV simulations are based on the 2004 Toyota Prius model that uses the split powertrain system with an Atkinson engine, a permanent magnet motor, and a nickel-metal hydride (NiMH)

[4] We model allocation of vehicles to drivers as a dictated assignment based on driver daily travel distance and do not model market mechanisms. As such, we find the best possible outcome for GHG emissions, which is a lower bound for market-based outcomes.

[5] We excluded data entries of public transportation and also excluded drivers who traveled zero miles or more than 200 miles. We fit the distribution to the reported distance traveled on the survey day with the assumptions of (1) the survey data are representative of the population, and (2) the distance driven on the survey day is the same distance driven every day for that vehicle.

[6] The deviation between data and the exponential fit in the 0-4 mile region has little effect on results because 0-4 mile trips contribute little to the social objectives in this study (the curves in Figure 5(d), (e) and (f))

battery pack. To account for structural weight needed to carry heavy battery packs, we include an additional 1 kg of structural weight per 1 kg of battery and motor weight. We created a comparable conventional vehicle (CV) model using a conventional powertrain and four-cylinder engine based on the Honda Accord to account for larger engine torque and power requirements, and the parameters that define the frontal area, drag coefficient and base weight are adjusted to match the Prius for fair comparison. The vehicle configuration parameters are included in Table A1 in the Appendix.

For the PHEV design, the Prius engine size is scaled by the peak power output from the base engine (57 kW) using a linear scaling algorithm. Similarly, the motor is scaled from the base motor (52 kW) linearly. Both the engine and motor weights are also scaled proportionally to the peak power. We use the Saft Li-ion battery module in the PSAT package for the PHEV energy storage device. Each cell in the module weighs 0.378 kg, with a modified specific energy of 100 Wh/kg and has a battery cell energy capacity of 21.6 Wh with a nominal output voltage of 3.6 volts. The weight of each 3-cell module is 1.42 kg after accounting for a packaging factor of 1.25. The battery size and capacity are scaled by specifying the number of cells in the battery pack. We assume an 800W base electrical hotel load on the PHEV, the HEV and the CV. To estimate the performance of a PHEV, we use the U.S. Environmental Protection Agency's Urban Dynamometer Driving Schedule (UDDS) driving cycle [18] to calculate simulated electrical efficiency (miles/kWh) in CD-mode for PHEVs, and gasoline efficiency (mpg) in CS-mode for PHEVs as well as for HEVs and CVs. We also perform a simulated performance test to calculate the time required to accelerate the vehicle from 0 to 60 miles per hour (mph) in the CD-mode and in the CS mode.[7]

Because the petroleum consumption, cost, and GHG emissions per mile associated with HEVs and CVs are independent of the number of miles driven per day, we focus on PHEV design and take the HEV and CV to have fixed designs. The HEV design is identical to the Prius model, which has a configuration of peak engine power 57 kW, motor power 52 kW, NiMH battery size 168 cells (1.3 kWh), fuel efficiency 60.1 miles per gallon, and 0-60 mph acceleration time 11.0 seconds. Similarly, our CV has an engine size 126 kW and fuel efficiency 29.5 miles per gallon, and 0-60 mph acceleration time 11.0 seconds. For the PHEVs, the design variables x consist of the engine scaling factor x_1, motor scaling factor x_2, battery pack scaling factor x_3, and battery SOE swing x_4. To reduce computational time and support global optimization, we created a set of polynomial meta-model fits as functions of $\mathbf{x}$ for the PHEV using discrete simulation data points: (1) CD-mode electricity efficiency η_E (mile per kWh); (2) CS-mode fuel efficiency η_G (mile per gallon); (3) CD-mode 0-60 mph acceleration time t_{CD} (second); (4) CS-mode 0-60 mph acceleration time t_{CS} (second); (5) CD-mode battery energy processed (charging and discharging) per mile μ_{CD} (kWh/mile); (6) CS-mode battery energy processed per mile μ_{CS} (kWh/mile); and (7) final SOC after multiple US06 aggressive driving cycles in CS mode u_{CS} (starting at the target SOC). Metamodels of η_E and η_G are used to calculate energy consumption; t_{CD} and t_{CS} are used to ensure comparison of equivalent-performance vehicles; μ_{CD} and μ_{CS} are usd to calculate battery degradation, and u_{CS} is used to ensure the engine is capable of providing average power needs in CS mode. We evaluated the four output values using PSAT over a grid of values for the inputs x_1={30, 45, 60}/57, x_2={50, 70, 90, 110}/52, x_3={200, 400, 600, 800, 1000}/1000 and multivariate polynomial functions were fit to the data using least squares.[8] The general form of the cubic fitting function f_{m3} is defined as (the subscript 3 indicates the PHEV case, which will be discussed later).

$$\begin{aligned} f_{m3}(\mathbf{x}) &= a_{m1}x_1^3 + a_{m2}x_2^3 + a_{m3}x_3^3 + a_{m4}x_1^2 + a_{m5}x_1x_2^2 \\ &+ a_{m6}x_1^2x_3 + a_{m7}x_1x_3^2 + a_{m8}x_2^2x_3 + a_{m9}x_2x_3^2 + a_{m10}x_1x_2x_3 \\ &+ a_{m11}x_1^2 + a_{m12}x_2^2 + a_{m13}x_3^2 + a_{m14}x_1x_2 + a_{m15}x_1x_3 \\ &+ a_{m16}x_2x_3 + a_{i17}x_1 + a_{m18}x_2 + a_{m19}x_3 + a_{m20} \end{aligned} \quad (4)$$

where the a_m terms are the coefficients for function m. The polynomial fitting coefficients for η_E, η_G, t_{CD}, t_{CS}, μ_{CD}, μ_{CS} and u_{CS} are listed in Table A1 in Appendix.[9] The maximum metamodel error among the test points is 0.1 miles/kWh, 0.1 miles/gallon, 0.5 seconds, 0.02 kWh, and 0.5% for electrical efficiency, gasoline efficiency, acceleration time, energy processed, and final SOC, respectively.

2.3 Electric Travel and Battery Degradation

To calculate each objective function, we first define the distance driven on electric power s_E and the distance driven on gasoline s_G as a function of the vehicle's AER s_{AER} and the total distance driven per day s. Assuming one charge per day, s_E and s_G are given by

$$\begin{aligned} s_E(\mathbf{x}, s) &= \begin{cases} s & \text{if } s \le s_{AER} \\ s_{AER}(\mathbf{x}) & \text{if } s > s_{AER} \end{cases} \\ s_G(\mathbf{x}, s) &= \begin{cases} 0 & \text{if } s \le s_{AER} \\ s - s_{AER}(\mathbf{x}) & \text{if } s > s_{AER} \end{cases} \end{aligned} \quad (5)$$

For PHEVs, we assume that the battery is charged to max SOC once per day. For HEVs and CVs, there is no electrical travel; thus HEV and CV can be seen as special cases with s_{AER}=0, so that s_E=0 and s_G=s. Assuming constant efficiency η_E (mile per kWh) in CD-mode, the AER of a PHEV can be calculated from the energy capacity per battery cell κ=0.0216 kWh/cell, the (scaled) number of cells x_3, and the design swing x_4:

$$s_{AER}(\mathbf{x}) = \kappa(1000x_3)x_4\eta_E \quad (6)$$

[7] Our simulation results are generally optimistic for all vehicles in that they do not account for factors such as vehicle wear, improper maintenance and tire pressure, aggressive driving cycles, extremely electric accessory loadings, or terrain and weather variation.

[8] SOE design swing specification (x_4) is not relevant for these performance tests.

[9] We truncated the acceleration data points greater than 13.0 seconds to improve the metamodel fit, and fit μ_{CD}, μ_{CS} and u_{CS} using quadratic terms to avoid over-fitting.

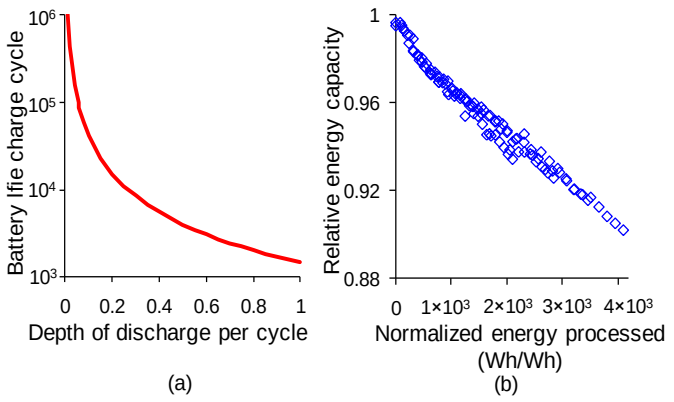

Figure 4. (a) Rosenkranz DOD-based degradation model; (b) Peterson energy-based degradation model

We consider two distinct battery degradation models from the literature and examine their implications for PHEV design. The Rosenkranz model [12], which has been used in prior PHEV studies [10-13], views battery degradation as a function of DOD per charge cycle, as shown in Figure 4 (a), which cannot predict additional degradation due to energy use in CS mode. In contrast, the Peterson model [14] was constructed by cycling modern A123 $LiFePO_4$ cells under representative driving cycles (non-constant C-rate) and measuring capacity fade as a function of energy processed, including intermediate charging and discharging over the driving cycle.[10] Results show relative energy capacity fade as a linear function of normalized energy processed while driving and while charging, as shown in Figure 4 (b).

Peterson model: The daily energy processed while driving w_{DRV} and charging w_{CHG} a PHEV can be expressed as

$$w_{DRV}(\mathbf{x},s)=\mu_{CD}s_E+\mu_{CS}s_G;\quad w_{CHG}(\mathbf{x},s)=\frac{s_E}{\eta_E\eta_B} \tag{7}$$

where μ_{CD} and μ_{CS} are energy processed per mile (kWh/mile) in CD and CS mode, respectively, and η_B is battery charging efficiency 95%. We assume that energy processed for daily charging is equal to net energy consumed in electrical travel per day. The relative energy capacity decrease can be calculated by the energy processed in driving and charging per cycle per cell per original cell energy capacity:

$$r_P(\mathbf{x},s)=\frac{\alpha_{DRV}w_{DRV}+\alpha_{CHG}w_{CHG}}{(1000x_3)\kappa} \tag{8}$$

where α_{DRV} = 3.46×10^{-5} and α_{CHG} = 1.72×10^{-5} are the coefficients for relative energy capacity fade. These coefficients are derived from the same data set described in [14].[11] If the battery end-of-life is defined as the point when the drop in relative energy capacity is r_{EOL}, the battery life θ_{BAT}, measured in days (or, equivalently, cycles), can be calculated as

$$\theta_{BAT}(\mathbf{x},s)=\frac{r_{EOL}}{r_P}=\frac{1000x_3\kappa r_{EOL}}{\alpha_{DRV}(\mu_{CD}s_E+\mu_{CS}s_G)+\alpha_{CHG}s_E(\eta_E\eta_B)^{-1}} \tag{9}$$

The r_{EOL} criterion is defined at 20% [14] .

Rosenkranz model: To estimate battery life using the Rosenkranz model, DOD needs to be calculated first. Because we assume energy consumption is constant in CD-mode, energy consumption is proportional to electric travel distance. If we define maximum SOC at 100%, the energy-based DOD δ is equal to the ratio of electric travel distance s_E to the maximum distance that could be traveled on total battery energy capacity:

$$\delta(\mathbf{x},s)=x_4\frac{s_E}{s_{AER}}=\frac{s_E}{\eta_E(1000x_3\kappa)} \tag{10}$$

The battery life charge cycle θ_{BAT} is estimated using the degradation curve in Figure 4 (a):

$$\theta_{BAT}(\mathbf{x},s)=1441\delta^{-1.46}=1441\left(\frac{s_E}{\eta_E(1000x_3\kappa)}\right)^{-1.46} \tag{11}$$

2.4 Objective Functions

The three objectives, net petroleum consumption, GHG emissions, and cost, are functions of vehicle design variables **x** and the distance traveled per day *s*. We define the functions as follows:

Petroleum consumption: The average petroleum consumed per day $f_G(\mathbf{x},s)$ is given by

$$f_G(\mathbf{x},s)=\frac{s_G(\mathbf{x},s)}{\eta_G(\mathbf{x})} \tag{12}$$

For the HEV and CV cases, Eq. (12) reduces to s/η_G.[12]

Life cycle greenhouse gas emissions: The operating (use phase) GHG emissions v_{OP} represents the average GHG emissions in kg CO_2 equivalent (kg-CO_2-eq) per day associated with the lifecycle of gasoline and electricity used to propel the vehicle:

$$v_{OP}(\mathbf{x},s)=\frac{s_E(\mathbf{x},s)}{\eta_E(\mathbf{x})}\frac{v_E}{\eta_C}+\frac{s_G(\mathbf{x},s)}{\eta_G(\mathbf{x})}v_G \tag{13}$$

where η_C=88% for battery charging efficiency [20], v_E = 0.752 kg-CO_2-eq per kWh for electricity emissions[13], and v_G = 11.34 kg-CO_2-eq per gallon for gasoline life cycle emissions. Total life cycle GHG emissions further includes the GHGs associated with production of the vehicle and battery. The average total lifecycle GHG emissions per day $f_V(\mathbf{x},s)$ is

$$f_V(\mathbf{x},s)=v_{OP}(\mathbf{x},s)+\frac{v_{VEH}}{\theta_{VEH}(s)}+\frac{v_{BAT}}{\theta_{BRPL}(\mathbf{x},s)} \tag{14}$$

where $\theta_{VEH}=s_{LIFE}/s$ is the vehicle life in days, s_{LIFE} = 150,000 miles[14] is the vehicle life in miles, θ_{BRPL} is the battery

[10] Deep discharging cycles may cause power fade in Li-ion battery cell [15], which we ignore in this study.

[11] The regression in [14] focused on finding the degradation from energy arbitrage, but in this paper the regression variables were chosen to enable predictions about degradation due to driving and recharging.

[12] Petroleum makes up less than 1.6% of the U.S. electricity grid mix [19], and we ignore it here.

[13] The life cycle GHG emissions of electricity is estimated based on the average emissions 0.69 kg-CO_2-eq/kWh of the US grid mixture [21] with 9% transmission loss [22].

[14] We assume that all vehicles must be replaced every 150,000 miles, which represents the U.S. average vehicle life [23]. This assumption may be unrealistic for vehicles driven very short or very long daily distances because

replacement effective life (defined below), $v_{BAT} = 1000x_3\kappa v_B$ is battery pack manufacturing emissions, v_B = 120 kg-CO_2-eq per kWh for Li-ion battery and 230 kg-CO_2-eq per kWh for NiMH battery is the life cycle GHG emissions associated with battery production, v_{VEH} = 8,500 kg-CO_2-eq per vehicle is the life cycle GHG emissions associated with vehicle production (excluding emissions from battery production) [2].

Battery replacement scenarios: We consider two battery replacement scenarios. The first is *battery leasing*: batteries are assumed to be replaced at the rate that they reach end of life, regardless of vehicle life. This simple and optimistic case essentially assumes that used batteries can be swapped from vehicle to vehicle until they reach end of life, and $\theta_{BRPL} = \theta_{BAT}$.

The second scenario is *buy-lease*: If the battery outlasts the life of the vehicle, a single battery pack must be purchased – partial payment for batteries is not allowed, and old batteries are not placed into new vehicles. But if the vehicle outlasts the battery, battery replacement is managed by lease. In this scenario, $\theta_{BRPL} = \min(\theta_{BAT}, \theta_{VEH})$.

Equivalent annualized cost (EAC): To calculate EAC, we define a nominal discount rate r_N, an inflation rate r_I, and the real discount rate $r_R = (1+r_N)/(1+r_I) - 1$ [24]. The net present value P of vehicle ownership is the sum of the cost of vehicle operation, vehicle production, and battery costs over the vehicle life:

$$P = \sum_{n=1}^{T(s)} \frac{c_{OP} D}{(1+r_R)^n} + c_{VEH} + \begin{cases} \text{Buy:} & c_{BAT} \\ \text{Lease:} & \sum_{n=1}^{T(s)} \frac{c_{BAT} R(r_N, B(\mathbf{x},s))}{(1+r_N)^n} \end{cases} \quad (15)$$

where D is driving days per year (D = 300 days in this study), T is vehicle life in years ($T(s) = \theta_{VEH}/D = s_{LIFE}/(sD)$), B is battery life in years ($B(\mathbf{x},s) = \theta_{BAT}(\mathbf{x},s)/D$). The operating cost per day c_{OP} is the sum of the cost of electricity needed to charge the battery and the cost of gasoline consumed:

$$c_{OP}(\mathbf{x},s) = \frac{s_E(\mathbf{x},s)}{\eta_E(\mathbf{x})} \frac{c_E}{\eta_C} + \frac{s_G(\mathbf{x},s)}{\eta_G(\mathbf{x})} c_G \quad (16)$$

R is capital recovery factor as a function of discount rate r and time period N in year [24]:

$$R(r,N) = \left(\sum_{n=1}^{N} \frac{1}{(1+r)^n} \right)^{-1} = \frac{r}{1-(1+r)^{-N}} \quad (17)$$

The net present value of battery leasing cost is calculated by calculating the EAC of the battery over its life B using $R(r_N, B)$ and then summing the present value of annual battery cost over the vehicle life T. The EAC of vehicle ownership is $P^*R(r_N,T(s))$. We divide by D to obtain EAC per driving day:

$$\begin{aligned} f_C(\mathbf{x},s) &= P \cdot R(r_N, T(s)) \cdot D^{-1} \\ &= c_{OP} \frac{R(r_N,T(s))}{R(r_R,T(s))} + c_{VEH} R(r_N,T(s)) D^{-1} \\ &\quad + \begin{cases} \text{Buy:} & c_{BAT} R(r_N,T(s)) D^{-1} \\ \text{Lease:} & c_{BAT} R(r_N, B(\mathbf{x},s)) D^{-1} \end{cases} \end{aligned} \quad (18)$$

The vehicle cost (excluding battery pack) c_{VEH} is the sum of vehicle base cost c_{BASE} = \$11,183, engine cost $c_{ENG}(x_1)$ = $17.8\times(57x_1)$ + 650, and motor cost $c_{MTR}(x_2)$ = $26.6\times(52x_2)$ + 520 [25].[15] The battery pack cost $c_{BAT} = 1000x_3\kappa c_B$, where Li-ion battery unit cost c_B = \$400/kWh (for PHEV only), and NiMH battery unit cost = \$600/kWh (for HEV only) in our base case [29].[16] We use the 2008 annual average residential electricity price c_E = \$0.11 per kWh [31], and the 2008 annual average gasoline price c_G = \$3.30 per gallon [32] in our base case. For HEV and CV, $s_E = 0$, and operating cost consists only of gasoline cost. We ignore the possibility of vehicle to grid energy arbitrage for PHEVs, since net earning potential is estimated to be low [33], especially under a mass adoption scenario. In the base case of this study, we assume zero discounting. By applying l'Hôpital's rule, the capital recovery factor reduces to $1/N$:

$$\lim_{r\to 0} \frac{r}{1-(1+r)^{-N}} = \lim_{r\to 0} \frac{1}{N(1+r)^{-N-1}} = \frac{1}{N} \quad (19)$$

Thus Eq. (18) can be simplified to

$$\begin{aligned} f_C(\mathbf{x},s) &= c_{OP} + c_{VEH}(TD)^{-1} + \begin{cases} \text{Buy:} & c_{BAT}(TD)^{-1} \\ \text{Lease:} & c_{BAT}(BD)^{-1} \end{cases} \\ &= c_{OP}(\mathbf{x},s) + \frac{c_{VEH}(\mathbf{x})}{\theta_{VEH}(s)} + \frac{c_{BAT}(\mathbf{x})}{\theta_{BRPL}(\mathbf{x},s)} \end{aligned} \quad (20)$$

The above equation has the same structure as the average lifecycle GHG function $f_V(\mathbf{x},s)$ in Eq. (14).

2.5 Constraint Functions

To ensure fair comparison, we require that all vehicles meet a minimum acceleration constraint of 0-60 mph in less than 11 seconds. Because we have limited our scope to all-electric PHEVs, we require the acceleration constraint to be satisfied both in CD mode, using electric power alone, and in CS mode, where the gasoline engine is also used. The resulting constraints are $t_{CD}(\mathbf{x}) \le 11$s and $t_{CS}(\mathbf{x}) \le 11$s. Additionally, we require the gasoline engine to be large enough to provide

other time-based factors also play a role in vehicle deterioration. However, these factors are only significant for regions of the objective function's integrand that are relatively insignificant to the integrated objective function, and they do not provide a significant source of error.

[15] To obtain a comparable vehicle base cost c_{BASE} (excluding engine, motor and battery) among PHEV, HEV and CV, we use the 2008 Prius manufacturer suggested retail price (MSRP) \$21,600 and subtract a 20% dealer mark-up [26], a NiMH battery pack of \$3,250, base engine cost \$1,665 and base motor cost \$1,902 in our cost estimation. We assume 20% dealer mark-up for the Prius NiMH battery replacement cost \$3,900 [27].The engine and motor costs are estimated using a cost model from the literature [13] and converted into 2008 dollars using the producer price index [28]. The resulting vehicle base cost is c_{BASE} = \$11,183. We ignore vehicle and battery salvage value.

[16] Future battery costs are uncertain. The Li-ion battery cost \$400/kWh [29] and NiMH battery cost \$600/kWh [30] are chosen to represent an optimistic but realistic estimate of near term battery costs in mass production, and we examine a range of costs in our sensitivity analysis.

average power for the vehicle in CS mode under an aggressive US06 driving cycle while maintaining the target SOC level in the battery. The resulting constraint is $u_{CS}(\mathbf{x}) \geq 32\%$. Finally, we impose simple bounds on the decision variables: $30/57 \leq x_1 \leq 60/57$, $50/52 \leq x_2 \leq 110/52$, $200/1000 \leq x_3 \leq 1000/1000$, $0 \leq x_4 \leq 0.8$ to avoid metamodel extrapolation. Any active simple bounds would imply a modeling limitation rather than a physical optimum. As we will later show, across all cases, of the simple bounds only the upper bounds on battery size and swing are ever active. The upper bound on battery size is reached only when minimizing petroleum consumption, since more battery is always preferred for this objective. The upper bound on swing is taken as a practical constraint since (1) SOC cannot be measured precisely, so the battery must be held safely away from the physical capacity, where explosion can occur, (2) battery resistance, which is relatively flat over most of the SOC window, rises considerably near 0% SOC, causing a drop in efficiency and power output and an increase in heat generation, and (3) batteries are typically considered "dead" when their usable capacity fades to 80% of original capacity.

3. RESULTS AND DISCUSSION

We use the Peterson battery degradation model (Eq. (8)), the buy-lease battery replacement scenario (θ_{BRPL}= min(θ_{BAT}, θ_{VEH})), and two driver segments (n=2) as our base case. We reformulate the problem into a factorable algebraic nonconvex mixed-integer nonlinear programming (MINLP) model[17] that can be solved using the GAMS/BARON convexification-based branch-and-reduce algorithm [35].

3.1 Optimal Solutions

The optimal vehicle type, design and allocation ranges for each case are summarized in Table 1. The performance values of CV and HEV are included in the first two columns of Table 1 for comparison. To further examine the optimal solutions, we plot the following function values at the optimal solution $\mathbf{x}^*$ as a function of driving distance per day in Figure 5: (1) life cycle equivalent cost, GHG emissions and petroleum consumption per-mile $f_O(\mathbf{x}^*,s)/s$; and (2) the population-weighted equivalent cost, GHG emissions and petroleum consumption per day $f_O(\mathbf{x}^*,s)\cdot f_S(s)$. The area under the population-weighted curve is the objective function. In each case, we compare the CV and HEV performance with the optimal PHEV design.

The optimal solution for minimum petroleum consumption reduces to a single PHEV87 design with the maximum allowed battery size allocated to all drivers.[18] Such a solution is expected since a large-capacity PHEV can travel long distances without using gasoline. Figure 5(a) shows the petroleum consumption per mile with respect to daily driving distance. No gasoline is consumed for driving distances under the AER of 87 miles. The $f_F(\mathbf{x}^*,s)\cdot f_S(s)$ plot in Figure 5(d) illustrates that moving all drivers from the CV to a the PHEV87 reduces net petroleum consumption per person per day (the area under the curve) by 96%.

The optimal solution for minimum GHG emissions is to allocate a medium-range PHEV40 to drivers who can charge every 87 miles or less (92% of drivers and 72% of VMT per day) and allocate a shorter-range PHEV25 to drivers who charge less frequently. There are two intersection points between the two PHEV GHG curves in Figure 5(b), and the optimal single cutoff point is located at the first intersection.[19] Although the PHEV40 GHG curve surpasses the PHEV25 after 87 miles, the difference between two is almost indistinguishable, and the portion of the population driving greater than 87 miles/day is small. Assigning all drivers high-AER PHEVs can significantly reduce petroleum consumption, but medium-AER PHEVs reduce the number of underutilized batteries in these vehicles, reducing the emissions associated with battery production as well as the emissions associated with reduced vehicle efficiency caused by carrying heavy batteries. While the most vehicles travel short distances each day (Figure 3), the majority of the GHG emissions are produced by those vehicles that travel 25- 45 miles/day (Figure 5(e)). A substantial reduction in GHG emissions is achieved by allocating PHEVs to drivers rather than HEVs or CVs, and a modest additional gain is possible by segmenting the population and allocating the right PHEV to the right driver.

Table 1. Optimization results for minimum fuel, petroleum, and GHG emissions objectives

Optimization Objective			Minimum Petroleum	Minimum GHGs		Minimum Cost	
Optimal Vehicle Set	CV	HEV	PHEV	PHEV	PHEV	PHEV	HEV
Allocation (miles)	0-200	0-200	0-200	0-87	87-200	0-51	51-200
AER (miles)	–	–	87	40	25	34	–
Engine power (kW)	126	57	47	47	43	46	57
Motor power (kW)	–	52	81	71	73	70	52
Battery cells	–	168	1000†	435	269	376	168
Battery design swing	–	–	0.8†	0.8†	0.8†	0.8†	–
Battery capacity (kWh)	–	1.3	21.6	9.4	5.8	8.1	1.3
CD eff. (miles/kWh)	–	–	5.05	5.29	5.35	5.31	–
CS eff. (mpg)	29.5	60.1	58.1	60.0	60.7	60.3	60.1
CD accel. (sec)	–	–	11.0	11.0	11.0	11.0	–
CS accel. (sec)	11.0	11.0	9.0	9.1	10.3	9.4	11.0
Final SOC	–	–	0.32	0.32	0.32	0.32	–
Petroleum (gallon per person-day)	1.12	0.55	**0.04**	0.18		0.32	
GHGs (kg-CO_2-eq per person-day)	14.6	8.20	8.12	**7.77**		7.91	
Cost ($ per person-day)	6.82	5.26	6.22	5.60		**5.21**	
Reduction from CV %	–	–	−96%	−47%		−24%	

†Variable limited by model boundary

[17] The detailed reformulation is presented in a companion paper focusing global optimization formulation and methodological contributions [34].

[18] We use the notation PHEVx to denote a PHEV with an AER of x miles.

[19] More intersection points are needed (n>2) to identify more than two vehicle regions.

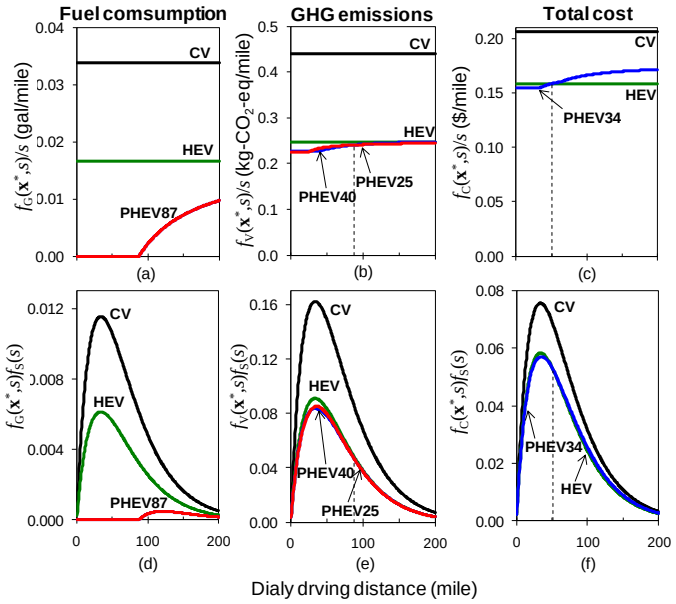

Figure 5. Optimal PHEV design and allocations for minimizing petroleum consumption, life cycle cost, and GHG emissions for the base case scenario

The minimum cost solution in the base case is to assign PHEV34s to drivers who can charge 51 miles or less (78% of drivers and 44% of VMT/day) and assign ordinary HEVs to drivers who charge less frequently. Figure 5(c) shows notable differences in cost trends among the two vehicles. However, when population weighting is included, the $f_C(\mathbf{x}^*,s)\cdot f_S(s)$ curves in Figure 5(f) reveals that the gap in net cost between the HEV and optimized PHEVs is small. Hence we conduct a series of sensitivity analyses to examine the minimum cost solutions under various scenarios.

An important observation on the optimal PHEV designs is that the optimal battery design swing for all three objective functions is the upper bound: 80%. The degradation mechanism based on energy-processed implies that for minimum life cycle cost, GHG emissions and petroleum consumption, designers should allow the maximum possible range of the battery to be used, even though this will require battery replacement for some drivers.

3.2 Sensitivity analyses

We conduct sensitivity analyses to examine the minimum cost solutions for various scenarios, which include: (1) single-vehicle allocation model, (2) three-vehicle allocation model, (3) battery leasing scenario, (4) Rosenkranz battery degradation model, (5) low Li-ion battery cost \$250/kWh, (6) high Li-ion battery cost \$1000/kWh, (7) low NiMH battery cost at \$440/ kWh, (8) high NiMH battery cost \$700/kWh, (9) low electricity price \$0.06/kWh, (10) high electricity price \$0.30/kWh, (11) low gasoline price at \$1.50 per gallon, (12) high gasoline price at \$6.0 per gallon, (13) carbon allowance price \$10 per metric ton of CO_2 equivalent (ton-CO_2-eq), (14) carbon allowance price \$100/ton-CO_2-eq, (15) nominal discount rate 5%, and (16) nominal discount rate 10%.[20] The optimal vehicle types and allocations for the sensitivity analyses are shown in Figure 6. The horizontal axis of the chart is the percentage of population covered by the allocated vehicles. The values of VMT percentage over the population and total equivalent cost per person per driving day are included for each optimal vehicle choice, and the cutoff daily mileage point is labeled where appropriate.

First, we tested sensitivity to the number of vehicle segments, examining the optimal solutions of single-vehicle and 3-vehcile allocation cases. For the single-vehicle case, ordinary HEV is the optimum choice for the entire range. The 3-vehice case shows that the range covered by PHEV34 in the base case is replaced by PHEV29 for the range of 0-33 miles and PHEV41 for the range of 33-54 miles. The allocation of HEV for longer driving distance is essentially not affected. Moreover, the minimum cost per person-day in the 3-vehicle case is only 0.2% lower than the base case, while the cost of the single-vehicle case is 1% higher. The results indicate that the two vehicle model in the base case is robust, and cases with more than three vehicles result in only minor improvements.

The battery leasing scenario does not change the optimal vehicle decisions in the base case because the optimized PHEV34 has a battery life shorter than vehicle life within 53 miles driving range, where buy-lease is equivalent to the leasing scenario ($\min(\theta_{BAT}, \theta_{VEH}) = \theta_{BAT}$). The Rosenkranz DOD-based degradation model, which encourages shallow swing to preserve battery life, results in a PHEV13 with 7.3 kWh battery at 32% SOE swing (a battery size equivalent to a PHEV32 with a 80% swing) for drivers below 24 miles/day and an HEV for the remainder. Thus, the best use strategy for PHEV batteries depends on the degradation mechanism. Planned PHEVs such as the Chevrolet Volt report a battery swing of around 50% in order to maintain battery life [36]. The Rosenkranz model is based on older battery technology, constant rate charge and discharge, and it cannot account for degradation in CS-mode. The latest data tested on $LiFePO_4$ cells with realistic driving cycles suggests that designers should consider using smaller battery packs with larger swing, even if the cost to replace the battery is accounted for.

The cases of high Li-ion battery cost, low gas price and high electricity price are not beneficial to PHEVs, and therefore the HEV is the low cost choice for all drivers in the range. The result of the low electricity price case shows that a PHEV40 has lower cost for most drivers, and the ordinary HEV remains preferable for long distance driving. Low electricity prices can be associated with off-peak charging; however, with high PHEV penetration and consequent demand for off-peak charging, off-peak rates will not remain as low. Similarly, lower battery costs or higher gasoline prices improve the economic performance of PHEVs and make them cost competitive for a wide range of drivers. We also examine two additional cases

[20] Among the 16 sensitivity analysis cases, the Rosenkranz and nominal discount rate cases are solved using local NLP solver with multi-start. The cost functions of these cases do not have closed-form expressions and require numerical integration.

with low and high HEV NiMH battery cost at $440/kWh and $700/kWh, respectively [30]. The result indicates the HEV allocation range varies between 42-200 and 58-200 miles, but PHEV is still the low-cost choice for the drivers with short to medium daily distances.

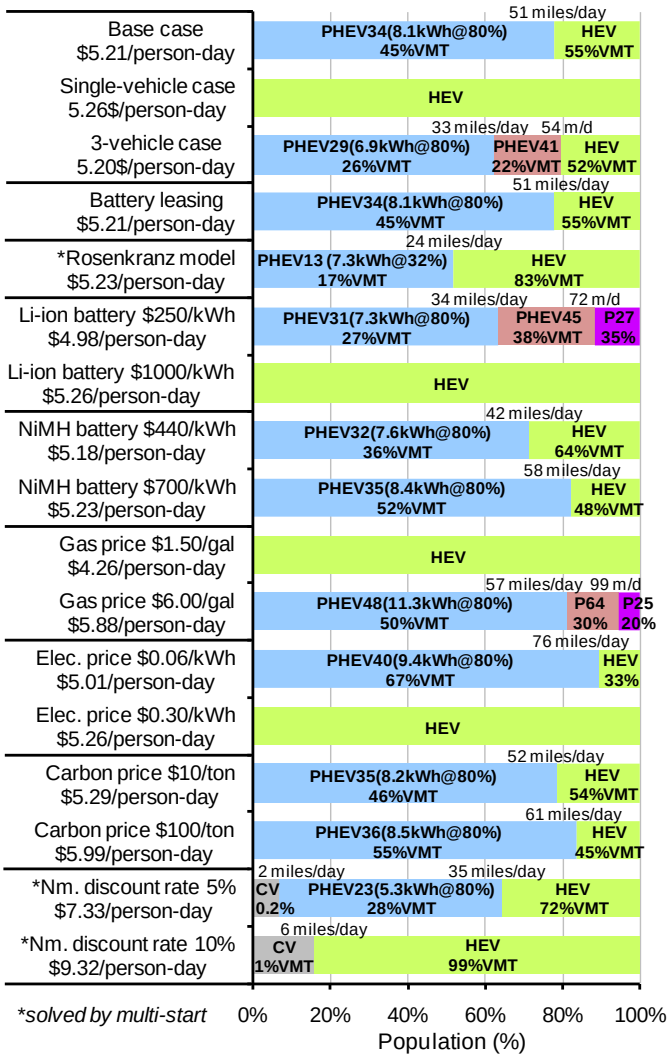

Figure 6. Optimal vehicle allocations for various scenarios. The base case assumes the buy-lease battery replacement scenario, the Peterson battery degradation model, $400/kWh Li-ion battery cost, $600/kWh NiMH battery cost, $3.30/gal gasoline, $0.11/kWh electricity, $0/ton CO_2-eq allowance price, and zero discounting

It is worth noting that we apply 3-vehcile models for solving the low Li-ion battery cost and high gas price cases. The reason is that we found dual-vehicle allocations result in a choice of low-AER PHEVs for longer driving distances to reduce weight of underutilized batteries, since a large number of miles are traveled beyond the AER. In these cases, the dual-PHEV cost curves have two intersection points, and the optimal cutoff is located at the second intersection point. In both cases with the 3-vehicle allocation model, the optimal solutions allocate medium-AER PHEVs to drivers with low daily driving distances, larger-AER PHEVs to driver have medium travel distance, and smaller PHEVs for the drivers who take long trips.

We examine the solution variations with two GHG allowance price levels, $10 and $100 per ton-$CO_2$-eq, by internalizing GHG emissions externalities to the cost objective function.[21] The carbon costs do not alter the vehicle design decisions significantly but extend the allocation range of PHEVs slightly. PHEV life cycle costs must already be comparable to HEV costs before carbon prices influence the least-cost solution.

The last two sensitivity analysis cases consider nominal discount rates r_N = 5% and 10% with an inflation rate r_I = 3%, the average from 2003-2008 [39]. A higher discount rate makes PHEVs less attractive relative to HEVs and CVs because the vehicle purchase cost paid upfront is higher, and fuel cost savings occur in the future. At a 5% discount rate, CV is the optimal choice for drivers who travel less than 2.4 miles per day. The optimal PHEV is a smaller 23-mile AER and covers 58% rather than 78% of the population on PHEV34s in the base case. At a 10% discount rate, PHEVs are not part of the least-cost solution, and HEV is the least cost alternative for 94% of population and 99% of VMT. It should be noted that the ranges covered by CV in these cases have lower population and VMT coverage than that in practice because the weighted frequencies in 0-4 miles are less than the ones in exponential fitting (Figure 3). At $400/kWh li-ion pack costs, PHEVs are part of the least cost solution for discount rates below 7%. At a 10% nominal discount rate, PHEVs are part of the least cost solution for battery pack prices below $300/kWh.

4. CONCLUSIONS

We construct an optimization model to determine optimal vehicle design and allocation of conventional, hybrid, and plug-in hybrid vehicles to drivers in order to minimize life cycle cost, petroleum consumption, and GHG emissions.

We find that (1) minimum petroleum consumption is achieved by assigning large capacity PHEVs to all drivers; (2) minimum life cycle GHG emissions are achieved by assigning PHEV40s to drivers who travel less than 87 miles/day (92% of drivers and 74% of VMT/day) and PHEV25s to drivers who travel further; and (3) minimum life cycle cost is achieved in our base case by assigning medium-range PHEV34s to drivers who travel less than 51 miles/day (78% of drivers and 45% of VMT/day) and HEVs to drivers who travel further. Optimal allocation of vehicles to drivers appears to be of second-order importance for net social cost and GHG emissions compared to an overall shift from CVs to HEVs or PHEVs. Additionally, life cycle costs of HEVs and PHEVs are comparable, particularly

[21] An externality cost study by the National Research Council estimated the range of environmental damage costs of carbon emissions as $10 to $100 per ton-$CO_2$-eq, with a middle estimate of $30 [37]. We examine the $10/ton and $100/ton cases, which also covers the 2020 carbon allowance prices of $20-$93/ton projected from the Waxman-Markey bill by the Department of Energy [38].

for drivers who charge frequently, and the least-cost solution is sensitive to the discount rate and the price of gasoline, electricity, and batteries. Relative to our base case of $3.30/gal gasoline, $0.11/kWh electricity, $400/kWh Li-ion batteries, $600/kWh NiMH batteries, and 0% discount rate PHEVs are part of the least-cost solution for gas prices above $3.03/gal, electricity prices below $0.14/kWh, battery prices below $460/kWh or nominal discount rates below 7%. Carbon allowance prices have marginal impact on optimal PHEV design or penetration, even at $100/ton. For example, when driven 34 miles per day, an HEV has life cycle emissions about 0.2 kg CO_2-eq/day greater than the PHEV34. A $100/ton allowance price translates to a $0.02/day penalty for the HEV relative to the PHEV35, which is about 0.4% of the equivalent daily cost of each vehicle. With the current average U.S. grid mix the relative incentive is small, even at high allowance prices. Decarbonization of the electricity grid is needed for allowance prices to be significant in PHEV competitiveness.

Using recent $LiFePO_4$ battery degradation models based on energy-processed in place of former DOD-based degradation models, we find that life cycle cost, GHG emissions and petroleum consumption are minimized by utilizing the maximum battery swing (80% in our model) and offering drivers a corresponding longer AER. This contrasts with current practice of restricting swing to values near 50% to improve battery life. Our results suggest that with $LiFePO_4$ cells, PHEV designers should optimally utilize full battery capacity and replace batteries as needed, rather than design unused battery capacity into the vehicle with the corresponding weight and cost implications. Allowing up to 80% swing rather than restricting swing to 50% reduces life cycle cost of PHEVs by 1%, GHGs by 2% and petroleum consumption by 65% in our model. Because cost implications are relatively small, other factors, such as logistics, customer satisfaction, and incentives, may play a significant role in determining battery swing in PHEV design. Current incentives for PHEVs, such as those outlined in the American Recovery and Reinvestment Act [40], provide subsidies based on battery size, rather than usable battery capacity or all-electric range. This creates a disincentive to increase swing because achieving a particular AER with a larger battery pack at lower swing will earn more incentives than achieving the same AER with a smaller battery pack at higher swing. Thus, PHEV subsidies would likely be better tied to PHEV AER, rather than battery capacity.

5. LIMITATIONS AND FUTURE WORK

The proposed model contains a number of assumptions that should be understood in order to interpret results meaningfully. These assumptions fall into four major categories: decision scope, driver behavior, technology scope, and endogeneity.

We examine a benevolent dictator's optimal choices of vehicle design and allocation to meet personal transportation needs in the U.S. with minimum equivalent daily cost, GHG emissions, or petroleum consumption. This scenario is useful for understanding the relationship between design / allocation and social objectives; however, market behavior may deviate. In particular, consumers may value purchase price over future petroleum cost savings with hyperbolic discounting, and they may value correlated vehicle attributes that are not considered here, such as convenience or interior space [41].

Secondly, we make several assumptions about driver behavior. While we account for across-driver heterogeneity in daily distance traveled, we lack data on within-driver variation. Accounting for this variation would be expected to increase petroleum consumption and GHG emissions from PHEVs slightly. Additionally, we assume each PHEV driver charges once per day, and we ignore the cost of charging infrastructure. Allowing multiple daily charges would require additional charging infrastructure and would give PHEVs a longer effective AER [42]. Finally, we use the UDDS cycle to estimate vehicle efficiency for all drivers, ignoring regional variation in driving style, terrain, weather, and grid characteristics [43-46]. In particular, our optimistic efficiency predictions may have implications for optimal battery pack sizing, and our use of average U.S. grid characteristics to calculate GHG emissions may over- or under-estimate emissions associated with particular regions and charge timing [46]. Future work will examine regional and marginal implications of PHEV charging time, location, and infrastructure.

The third class of modeling assumptions involves technology scope. We assume a fixed Li-ion battery technology for PHEVs with performance models based on a Saft cell and degradation data from A123 cells. In practice different battery designs may be used for different vehicle systems [10, 47, 48], and we leave such assessment for future work. We assume a static battery technology with a base cost of $400/kWh installed pack cost, intended to represent an optimistic but realistic future scenario, particularly for thick-electrode high-energy batteries used for larger packs [10, 29]. Dynamics of technology advancement and cost reduction could have strategic implications for vehicle system design and allocation [49]. We examine only energy-processed based degradation mechanisms and ignore calendar (storage) degradation mechanisms that affect batteries when not in use. Future work is needed to characterize these time-based mechanisms. We also limit our study to all-electric PHEVs. Blended-mode PHEVs that make use of the gasoline engine during CD-mode offer additional control flexibility and the ability to design vehicles with smaller motors and battery packs [50]. Analysis of blended-mode PHEVs requires examination of the space of control strategy variables, and we leave this for future work.

Finally, we treat gasoline prices and grid characteristics as exogenous factors. A significant shift to PHEVs may influence the price of gasoline, electricity, or batteries or the mix of electricity generation modes (because of new plant construction or increase in off-peak demand) [46]. We leave examination of these potentially endogenous relationships for future work.

ACKNOWLEDGMENTS

The authors would like to thank Prof. Jay Whitacre, Prof. Chris Hendrickson, and the members of the Design Decisions Laboratory, the Carnegie Mellon Green Design Institute and

xEV Group for their feedback and help with model formulation. This research was supported in part by the National Science Foundation's CAREER Award #0747911, a grant from the National Science Foundation program for Material Use, Science, Engineering and Society (MUSES): Award #0628084, and grants from Ford Motor Company and Toyota Motor Corporation. C.-S.S. gratefully acknowledges support from the Liang Ji-Dian Fellowship. S.B.P. gratefully acknowledges support from a Dowd Fellowship.

REFERENCES

[1] Bandivadekar, A., Bodek, K., Cheah, L., Evans, C., Groode, T., Heywood, J., Kasseris, E., Kromer, M., and Weiss, M., 2008, "On the Road in 2035: Reducing Transportation's Petroleum Consumption and GHG Emissions," LFEE 2008-05 RP, Massachusetts Institute of Technology, Cambridge, MA.

[2] Samaras, C., and Meisterling, K., 2008, "Life Cycle Assessment of Greenhouse Gas Emissions from Plug-in Hybrid Vehicles: Implications for Policy," Environmental Science & Technology, **42**(9), pp. 3170-3176.

[3] Bureau of Transportation Statistics, 2003, "National Household Travel Survey 2001", U.S. Department of Transportation.

[4] Bunkley, N., 2008, "Plug-in Hybrid from G.M. Is Nearly Ready for Testing", The New York Times, http://www.nytimes.com/2008/08/15/business/15volt.html.

[5] Toyota, 2009, "2010 Prius Plug-in Hybrid Makes North American Debut at Los Angeles Auto Show," http://pressroom.toyota.com/pr/tms/toyota/2010-prius-plug-in-hybrid-makes-149402.aspx

[6] Frank, A.A., 2007, "Plug-in Hybrid Vehicles for a Sustainable Future," American Scientist, **95**(2), pp. 158-165.

[7] Markel, T., Brooker, A., Gonder, J., M. O'Keefe, Simpson, A., and Thornton, M., 2006, "Plug-in Hybrid Vehicle Analysis," NREL/MP-540-40609, National Renewable Energy Laboratory, Golden, CO.

[8] Shiau, C.S.N., Samaras, C., Hauffe, R., and Michalek, J.J., 2009, "Impact of Battery Weight and Charging Patterns on the Economic and Environmental Benefits of Plug-in Hybrid Vehicles," Energy Policy, **37**(7), pp. 2653-2663.

[9] Hall, J.C., Lin, T., and Brown, G., 2006, "Decay Processes and Life Predictions for Lithium Ion Satellite Cells," *4th International Energy Conversion Engineering Conference and Exhibit (IECEC)*, 26-29, June 2006, San Diego, CA, AIAA 2006-4078.

[10] Kromer, M.A., and Heywood, J.B., 2008, "A Comparative Assessment of Electric Propulsion Systems in the 2030 Us Light-Duty Vehicle Fleet," SAE International Journal of Engines, **1**(1), pp. 372-391.

[11] Markel, T., and Simpson, A., 2006, "Plug-in Hybrid Electric Vehicle Energy Storage System Design," *Advanced Automotive Battery Conference*, May 17-19, 2006, Baltimore, Maryland

[12] Rosenkranz, K., 2003, "Deep-Cycle Batteries for Plug-in Hybrid Application," *EVS20 Plug-In Hybrid Vehicle Workshop*, Long Beach, CA

[13] Simpson, A., 2006, "Cost-Benefit Analysis of Plug-in Hybrid Electric Vehicle Technology," *Proceedings of the 22nd International Battery, Hybrid and Fuel Cell Electric Vehicle Symposium and Exhibition (EVS-22)*, October 23-28, 2006, Yokohama, Japan

[14] Peterson, S.B., Whitacre, J.F., and Apt, J., 2010, "Lithium-Ion Battery Cell Degradation Resulting from Realistic Vehicle and Vehicle-to-Grid Utilization," Journal of Power Sources, **195**(8), pp. 2385–2392.

[15] Belt, J.R., Ho, C.D., Motloch, C.G., Miller, T.J., and Duong, T.Q., 2003, "A Capacity and Power Fade Study of Li-Ion Cells During Life Cycle Testing," Journal of Power Sources, **123**(2), pp. 241-246.

[16] Federal Highway Administration, 2010, "National Household Travel Survey 2009," Department of Transportation, Washington, DC.

[17] Argonne National Laboratory, 2008, "Powertrain Systems Analysis Toolkit (PSAT)."

[18] Environmental Protection Agency, "Dynamometer Drive Schedules", http://www.epa.gov/nvfel/testing/dynamometer.htm.

[19] Energy Information Administration, 2009, "Electric Power Annual 2007", U.S. Department of Energy, DOE/EIA-0348(2007), http://www.eia.doe.gov/cneaf/electricity/epa/epa.pdf.

[20] EPRI, 2007, "Environmental Assessment of Plug-in Hybrid Electric Vehicles. Volume 1: Nationwide Greenhouse Gas Emissions," Electric Power Research Institute.

[21] Weber, C.L., Jaramillo, P., Marriott, J., and Samaras, C., 2010, "Life Cycle Assessment and Grid Electricity: What Do We Know and What Can We Know?," Environmental Science and Technology, **44**(6), pp. 1895–1901.

[22] Energy Information Administration, 2008, "Annual Energy Review 2007", U.S. Department of Energy, http://www.eia.doe.gov/emeu/aer/elect.html.

[23] Environmental Protection Agency, 2006, "Emission Durability Procedures and Component Durability Procedures for New Light-Duty Vehicles, Light-Duty Trucks and Heavy-Duty Vehicles; Final Rule and Proposed Rule", http://www.epa.gov/EPA-AIR/2006/January/Day-17/a074.pdf.

[24] Neufville, R., 1990, *Applied Systems Analysis: Engineering Planning and Technology Management*, McGraw-Hill, Inc., New York, New York.

[25] EPRI, 2001, "Comparing the Benefits and Impacts of Hybrid Electric Vehicle Options", Electric Power Research Institute.

[26] Lipman, T.E., and Delucchi, M.A., 2006, "A Retail and Lifecycle Cost Analysis of Hybrid Electric Vehicles," Transportation Research Part D-Transport and Environment, **11**(2), pp. 115-132.

[27] Naughton, K., 2008, "Assaulted Batteries", Newsweek, July 02, 2008, http://www.newsweek.com/id/138808.
[28] Bureau of Labor Statistics, 2009, "Producer Price Indexes," U.S. Department of Labor.
[29] Whitacre, J.F., 2009, "The Economics and Science of Materials for Lithium Ion Batteries and Pem Fuel Cells," Working Paper, Carnegie Mellon University, Pittsburgh, PA.
[30] Duvall, M., 2004, "Advanced Batteries for Electric-Drive Vehicles," Electric Power Research Institute, Palo Alto, CA,
[31] Energy Information Administration, 2009, "Average Retail Price of Electricity to Ultimate Customers: Total by End-Use Sector", U.S. Department of Energy, http://www.eia.doe.gov/cneaf/electricity/epm/table5_3.html.
[32] Energy Information Administration, 2009, "The U.S. Weekly Retail Gasoline and Diesel Prices", U.S. Department of Energy, http://tonto.eia.doe.gov/dnav/pet/pet_pri_gnd_dcus_nus_a.htm.
[33] Peterson, S.B., Whitacre, J.F., and Apt, J., 2010, "The Economics of Using Plug-in Hybrid Electric Vehicle Battery Packs for Grid Storage," Journal of Power Sources, **195**(8), pp. 2377-2384.
[34] Shiau, C.-S.N., and Michalek, J.J., 2010, "A Mixed-Integer Nonlinear Programming Model for Deterministic Global Optimization of Plug-in Hybrid Vehicle Design and Allocation," *ASME 2010 International Design Engineering Technical Conferences*, Montreal, Quebec, Canada.
[35] Tawarmalani, M., and Sahinidis, N.V., 2004, "Global Optimization of Mixed-Integer Nonlinear Programs: A Theoretical and Computational Study," Mathematical Programming, **99**(3), pp. 563-591.
[36] gm-volt.com, 2009, "Latest Chevy Volt Battery Pack and Generator Details and Clarifications," http://gm-volt.com/2007/08/29/latest-chevy-volt-battery-pack-and-generator-details-and-clarifications/
[37] National Research Council, 2009, *Hidden Costs of Energy: Unpriced Consequences of Energy Production and Use*, The National Academies Press, Washington, DC.
[38] Energy Information Administration, 2009, "Energy Market and Economic Impacts of H.R. 2454, the American Clean Energy and Security Act of 2009", Department of Energy, http://www.eia.doe.gov/oiaf/servicerpt/hr2454/pdf/sroiaf%282009%2905.pdf.
[39] US Bureau of Labor Statistics http://www.bls.gov/data/inflation_calculator.htm.
[40] U.S. Congress, 2008, "American Recovery and Reinvestment Act of 2009", http://fdsys.gpo.gov/fdsys/pkg/BILLS-111hr1ENR/pdf/BILLS-111hr1ENR.pdf.
[41] Allcott, H., and Wozny, N., 2009, "Gasoline Prices, Fuel Economy, and the Energy Paradox," Working Paper, MIT Department of Economics, Cambridge, MA.
[42] Bradley, T.H., and Frank, A.A., 2009, "Design, Demonstrations and Sustainability Impact Assessments for Plug-in Hybrid Electric Vehicles," Renewable and Sustainable Energy Reviews, **13**, pp. 115-128.
[43] Gonder, J., Markel, T., Simpson, A., and Thornton, M., 2007, "Using Gps Travel Data to Assess the Real World Driving Energy Use of PHEVs," *Transportation Research Board Annual Meeting*, Jan 21-25, 2007, Washington, D.C.
[44] Moawad, A., Singh, G., Hagspiel, S., Fellah, M., and Rousseau, A., 2009, "Impact of Real World Drive Cycles on PHEV Fuel Efficiency and Cost for Different Powertrain and Battery Characteristics," *The 24th International Electric Vehicle Symposium and Exposition (EVS-24)*, May 13-16, 2009, Stavanger, Norway
[45] Patil, R., Adornato, B., and Filipi, Z., 2009, "Impact of Naturalistic Driving Patterns on PHEV Performance and System Design," Working Paper, University of Michigan, Ann Arbor, MI.
[46] Sioshansi, R., and Denholm, P., 2009, "Emissions Impacts and Benefits of Plug-in Hybrid Electric Vehicles and Vehicle-to-Grid Services," Environmental Science & Technology, **43**(4), pp. 1199-1204.
[47] Albertus, P., and Newman, J., 2008, "A Simplified Model for Determining Capacity Usage and Battery Size for Hybrid and Plug-in Hybrid Electric Vehicles," Journal of Power Sources, **183**(1), pp. 376-380.
[48] Pesaran, A., Markel, T., Tataria, H., and Howell, D., 2007, "Battery Requirements for Plug-in Hybrid Electric Vehicles - Analysis and Rationale," *The 23th International Electric Vehicle Symposium (EVS-23)*, December 2-5, 2007, Anaheim, CA
[49] Struben, J., and Sterman, J.D., 2008, "Transition Challenges for Alternative Fuel Vehicle and Transportation Systems," Environment and Planning B-Planning & Design, **35**(6), pp. 1070-1097.
[50] Moura, S.J., Callaway, D.S., Fathy, H.K., and Stein, J.L., 2008, "Impact of Battery Sizing on Stochastic Optimal Power Management in Plug-in Hybrid Electric Vehicles," *IEEE International Conference on Vehicular Electronics and Safety, 2008*, September 22-24, Columbus, OH

APPENDIX

Table A1. Vehicle configurations in simulation

Module	Property	CV	HEV	PHEV
Vehicle body & chassis	F/R weight ratio		0.6/0.4	
	Drag coefficient		0.26	
	Frontal area (m^2)		2.25	
	Tire specs		P175/65 R14	
	Body mass (kg)		824	
Engine	Power (kW)	126	57	30-60
	Mass (kg)	296	114	50-110
Motor	Power (kW)	-	52	50-110
	Mass (kg)	-	65	40-143
Battery	No. of cells	-	168	200-1000
	Mass (kg)	-	36	60-419
Electrical accessory	Power (kW)	0.8	0.8	0.8
	Net weight (kg)	1709	1520	1497-1995

Table A2. Polynomial coefficients of the PHEV performance meta-model

f_{m3}	η_E	η_G	t_{CD}	t_{CS}	μ_{CD}^*	μ_{CS}^*	u_{CS}^*
m	1	2	3	4	5	6	7
a_{m1}	0.008	2.214	1.457	3.334			
a_{m2}	0.154	1.087	-5.496	-2.266			
a_{m3}	0.353	5.578	-28.46	-20.26			
a_{m4}	-0.005	-0.815	0.913	0.414			
a_{m5}	-0.005	0.510	-0.881	-3.524			
a_{m6}	-0.025	1.562	-1.050	-0.286			
a_{m7}	0.000	2.212	-0.308	-10.11			
a_{m8}	-0.057	-0.613	2.044	1.951			
a_{m9}	-0.043	0.254	15.61	10.31			
a_{m10}	-0.016	-0.159	0.336	5.808			
a_{m11}	-0.001	-8.906	-4.634	-6.932	0.010	0.466	-0.194
a_{m12}	-0.805	-6.095	31.48	15.80	0.011	-0.008	-0.005
a_{m13}	-0.656	-15.21	34.02	39.20	0.053	-0.018	0.047
a_{m14}	0.057	0.089	1.153	7.901	0.000	-0.014	0.000
a_{m15}	0.080	-3.274	1.169	6.582	0.008	-0.038	0.011
a_{m16}	0.342	2.498	-32.06	-30.12	-0.003	0.010	-0.001
a_{m17}	-0.191	2.622	3.405	-6.734	0.097	-0.890	0.382
a_{m18}	1.189	9.285	-54.47	-26.39	0.038	0.077	0.019
a_{m19}	-0.347	5.837	9.570	-4.098	0.370	0.400	-0.077
a_{m20}	4.960	57.68	44.23	32.10	2.196	1.441	0.140

* The terms are fit with quadratic form.